Numerical Study on the Transition Performance of a Scale Model Helicopter from Hovering to Vertical Autorotation

A. A. Wahab[♣] , M. S. M. Ali[♠]
Dept. of Aeronautical & Automotive Eng.,
Faculty of Mechanical Engineering,
University of Technology Malaysia
abas@fkm.utm.my, sukriali@gmail.com

Abstract: Autorotation characteristics for typical scale model helicopter in terms of induced velocity, rate of descent, main rotor rotational speed, thrust and torque were studied. Power-off after hovering manoeuvre was picked for a case of study because of their critical induced velocity state. Contribution in every blade element in the effect of thrust, torque and induced velocity has been taken in consideration by blade element momentum theory for better results. Newton second laws were used in kinematics analysis for enabling the rate of descent, helicopter acceleration and main rotor rpm to be prescribed. In this analysis, the results show all the autorotation characteristics fluctuated at the beginning then become constant at the end. This situation proved that transition from hovering to steady autorotation has been achieved.
Keyword: autorotation, hovering, kinematics, fluctuated

Nomenclature

a	lift slope, 1/rad	r	radial distance from the blade root, m
c	chord length, m	S	helicopter vertical manoeuvre distance, m
C_l	section lift coefficient	V_c	vertical velocity, downward positive, m/sec
C_d	section drag coefficient	v_h	hover induce velocity, m/sec
dr	length of small blade element, m	v_i	induce velocity, m/sec
I_R	rotor mass moment of inertia, kgm^2	W	helicopter weight, N
i	number of step iteration	θ	main rotor blade pitch angle, radian
N_b	number of blade	Ω	main rotor rotational speed, rad/sec
U	resultant velocity at blade element, m/sec		
U_P	out-of-plane velocity normal to rotor disk plane, m/sec		
U_T	in-plane velocity parallel to rotor disk plane, m/sec		

1. Introduction

The potential of Unmanned Aerial Vehicle (UAV) helicopter is almost undoubtedly. These vehicles are indispensable to manoeuvre in compact areas and to reduce human risk. These criterions are important to perform special task where regular vehicles do not have the necessary access. In military, the use of UAV are very vital for doing tasks such as aerial reconnaissance, covert imaging, battlefield management and damage assessment, that are predominant aspects of today defence strategies. In civil usage, the tasks are such as information and communication system, traffic control system, agricultural spreading and biochemical sensor. These new approach of activities are increasingly play important role in country development system planning.

UAV helicopter can be said reliable and safe if several flight tests shown good performance identification. In these flight tests, it bring together with expensive devices to perform its task. Although before the flight test, wind tunnel and computer simulation had been conducted, the risk to system failure is still high. Then, there is a possibility that expensive devices will damage because of high landing velocity impact. Fortunately, UAV helicopter has the ability to perform autorotation manoeuvre [1].

Autorotation is the continuous rotation of a body in an airstreams without the supply of external power [2]. When UAV helicopter in autorotation manoeuvre, airstreams from velocity descent was extracted by main rotor blade to

---

[♣] Prof, Dr, Ir.
[♠] MEng. student

provided sufficient power and thrust that needed. Therefore, it is important to prevent main rotor from decay rapidly [3]. The main factor of rotor decay is high decelerating torque compare to accelerating torque. This situation is depicted on autorotation blade region that there are stall and driven region constructed by decelerating torque and driving region constructed by accelerating torque [4].

Vertical autorotation is one of the critical flight conditions of a helicopter. This is because, helicopter prone to loss control due to unusual characteristics of the flow through and around the rotor [5]. These flow called vortex ring state for low descent and windmill brake state for fast descent. Under vortex ring state, the wake vorticity produced by blades cannot convect away from the rotor, and accumulates near the rotor plane, clumping together forming a flow condition that is analogous to flight in a vortex ring [6]. Because of unsteadiness of the rotor wake, vortex ring is unstable condition and easily burst to create new vortex ring.

Momentum theory is invalid in the vortex ring state because the flow can take on two possible directions and well defined slipstream ceases to exist. However, the induced velocity curve can still be defined approximately on the basis of flight test or other experiments [7]. Because of that, some modification on BEMT method by using non-uniform circularly symmetrical disk loading is needed to define the aerodynamics characteristics of helicopter in vertical autorotation analysis [8]. Then, thus characteristics will be used in determining the kinematics parameters of helicopter autorotation at any time.

2. Methodology

As results of all that, this paper described the autorotation characteristics of typical UAV helicopter from hovering condition to vertical autorotation manoeuvre. The scope of this study is emphasizing on main rotor blade aerodynamic without interrelated to others helicopter discipline. BEMT is used to predict the induced velocity and load distributions on every blade point. For the better results, best fit induced velocity curve by previous researcher has been used and non-uniform circularly symmetrical disk loading has been taken into consideration. In kinematics equation, one degree of freedom in the earth fixed coordinate system is used. In dynamics equation relation and calculations Second Newton law is widely used.

2.1 Blade Elements Momentum Theory

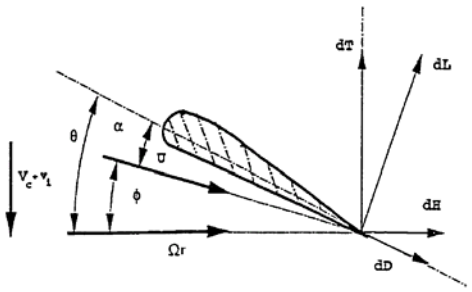

Fig.1 Incident velocities and aerodynamics environment at a typical blade element.

Figure 2.1 shows a sketch of the flow environment and aerodynamics forces at representative blade element on the rotor. The resultant velocity U at the blade element r is;

$$U = \sqrt{U_T{}^2 + U_p{}^2} \tag{1}$$

$$U_T = V_c + v_i \tag{2}$$

$$U_p = \Omega r \tag{3}$$

The resultant incremental lift dL and drag dD on this blade element are;

$$dL = \frac{1}{2}\rho U^2 c C_l dr \tag{4}$$

$$dD = \frac{1}{2}\rho U^2 c C_d \, dr \tag{5}$$

$$C_l = a\alpha \tag{6}$$

$$C_d = \delta_1 + \delta_2 \alpha + \delta_3 \alpha^2 \tag{7}$$

For NACA 0012 airfoil and Mach = 0.2

$a = 5.75$ per radian

$\delta_1 = 0.0087$, $\delta_2 = -0.021$, $\delta_3 = 0.4$

The relative inflow angle ϕ and effective angle of attack α is;

$$\phi = \tan^{-1}\left(\frac{U_P}{U_T}\right) \tag{8}$$

$$\alpha = \theta - \phi \tag{9}$$

Therefore, the contributions to the thrust dT, torque dQ, and power dP of the rotor on this blade element are;

$$dT = N_b (dL\cos\phi - dD\sin\phi) \tag{10}$$

$$dQ = N_b r (dL\sin\phi - dD\cos\phi) \tag{11}$$

$$dP = N_b \Omega r (dL\sin\phi - dD\cos\phi) \tag{12}$$

2.2 Induced Velocity

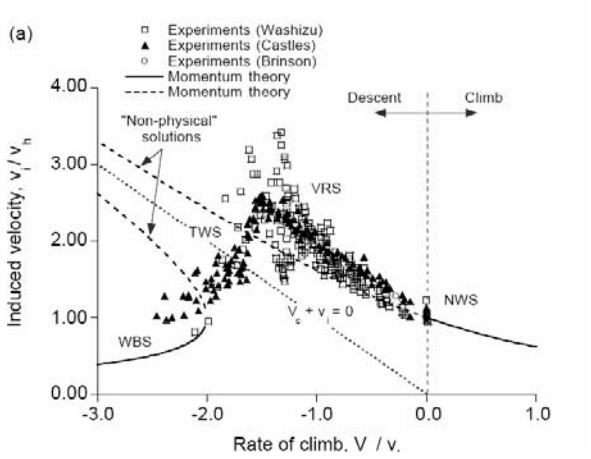

Fig. 2 Induced velocity curve by previous researcher.

Figure 2.2 shows the complete induced velocity curve for a rotor in axial flight. The flight regimes of interest for the vortex ring state is for $-2 \le {}^{V_c}\!/_{V_h} \le 0$ where momentum based aerodynamic theories are strictly invalid. An approximation to the measured curve by Leishman [7] gives;

The region $-2 \le {}^{V_c}\!/_{V_h} \le 0$;

$$v_i = 1.15v_h - 1.125v_h\left(\frac{v_c}{v_h}\right) - 1.372v_h\left(\frac{v_c}{v_h}\right)^2 - 1.718v_h\left(\frac{v_c}{v_h}\right)3 - 0.655v_h\left(\frac{v_c}{v_h}\right)^2 4 \tag{13}$$

The region $V_c/V_h \leq -2$

$$v_i = \left(\frac{-v_c}{2}\right) - \sqrt{\left(\frac{-v_c}{2}\right)^2 - {v_h}^2} \tag{14}$$

From momentum theorem hovering induced velocity v_h ;

$$v_h = \frac{-\frac{\Omega}{2} acN_b + \sqrt{\left(\frac{\Omega}{2} acN_b\right)^2 + 8\pi N_b \Omega^2 ra\theta c}}{8\pi} \tag{15}$$

2.3 Dynamics Equation

From Newtons second law, vertical force balance give;

$$ma = mg - T + D \tag{16}$$

From equation (4), (5) and (10) the total thrust T ;

$$T = \frac{1}{2}\rho U^2 cN_b \int_0^R (C_l \cos\phi - C_d \sin\phi) dr \tag{17}$$

The helicopter parasite drag D is defined by an equivalent flat plate area f as;

$$D = \frac{1}{2}\rho (V_c + v_i)^2 f \tag{18}$$

Where the value of flat plate area [8] is approximately $f = 1.2$

The torque balance equation can be expressed simply as;

$$I_R \dot{\Omega} = -Q \tag{19}$$

From equation (4), (5) and (11) the total torques Q;

$$Q = \frac{1}{2}\rho U^2 cN_b \int_0^R (C_l \sin\phi - C_d \cos\phi) r dr \tag{20}$$

2.4 Kinematical Relations

The instantaneous velocity is defined as the limit of the average velocity as the time interval approaches zero. Thus;

$$V = \lim_{\Delta t \to 0} \frac{\Delta S}{\Delta t}, a = \lim_{\Delta t \to 0} \frac{\Delta V}{\Delta t} \tag{21}$$

Then, the rate of descent at time t can be express as:

$$adt = dV \tag{22}$$

By using Euler method to this differential equation, the first order differential equation is:

$$\frac{dy}{dt} = f(y,t) \tag{23}$$

Then the method of numerical integration can be generalized to determine the function at $t = i + 1$

$$y_{i+1} = y_i + f(y_i, t_i)\Delta t \tag{24}$$

$$t_i = i\Delta t \tag{25}$$

Initial value constraints;

$$\begin{bmatrix} v_0 \\ y_0 \end{bmatrix} = \begin{bmatrix} 0 \\ 0 \end{bmatrix}, \begin{bmatrix} \Omega_0 \\ \theta_0 \end{bmatrix} = \begin{bmatrix} 0 \\ 0 \end{bmatrix} \tag{26}$$

Then the numerical solution becomes;

$$\begin{bmatrix} v_{i+1} \\ y_{i+1} \end{bmatrix} = \begin{bmatrix} \mathrm{v_i} + f(\mathrm{v_i}, \mathrm{y_i}, \mathrm{t_i})\Delta \mathrm{t} \\ \mathrm{y_i} + \mathrm{v_i}\Delta \mathrm{t} \end{bmatrix} \tag{27}$$

$$\begin{bmatrix} \Omega_{i+1} \\ \theta_{i+1} \end{bmatrix} = \begin{bmatrix} \Omega_\mathrm{i} + f(\Omega_\mathrm{i}, \theta_\mathrm{i}, \mathrm{t_i})\Delta \mathrm{t} \\ \theta_\mathrm{i} + \Omega_\mathrm{i}\Delta \mathrm{t} \end{bmatrix} \tag{28}$$

Where,

$$f(\mathrm{v_i}, \mathrm{y_i}, \mathrm{t_i}) = a_i \tag{29}$$

$$f(\Omega_\mathrm{i}, \theta_\mathrm{i}, \mathrm{t_i}) = \ddot{\Omega} \tag{30}$$

3. Results and Discussion

Table 1 Specification of typical helicopter in this analysis

specifications	Radius(m)	Chord(m)	Mass(kg)	I(kgm^2)	Ω_{Hover}(rad/sec)	θ_{Hover}(rad)	θ_{finalr}(rad)
Value	0.9144	0.1	6.413	2	72	0.14	0

The validity of the analysis presented in this paper here is examined by comparing steady rate of descent data by Slaymaker *et al.* [9]. Figure 3 shows the differential descent velocity value of a typical model from hovering to steady vertical autorotation. Using non uniform circularly loading method, steady descent velocity increase about 20 percent compare to uniform disk loading method by Slaymaker. This is because by assuming uniform disk loading, no contribution of induced velocity to angle of attack is taken into consideration; where the variation of angle of attack is inherently affecting thrust and torque. This is true when experiment had been done by same researcher shown, higher descent rate was achieved. This value is quite similar to non uniform method been used despite little deviation at the beginning.

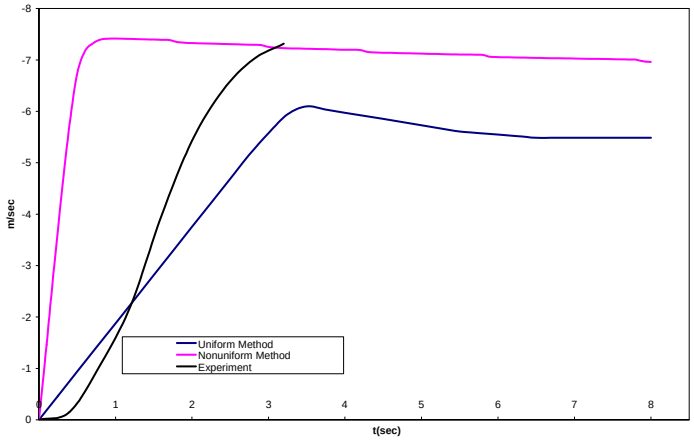

Fig.3 Graph data comparison with previous research.

After helicopter power-off, main rotor makes use of external force to keep rotating. The magnitude of this force is depended on how much torque been produced at certain collective pitch angle. Contribution only from blade momentums is not enough to support such amount of torque. Therefore, helicopter experienced rigorous rotor speed decay at the first few second until typical descent velocity value is reach; which can contribute to create driving force. This situation is revealed by figure 4 shows the torque distribution along blade span at certain time.

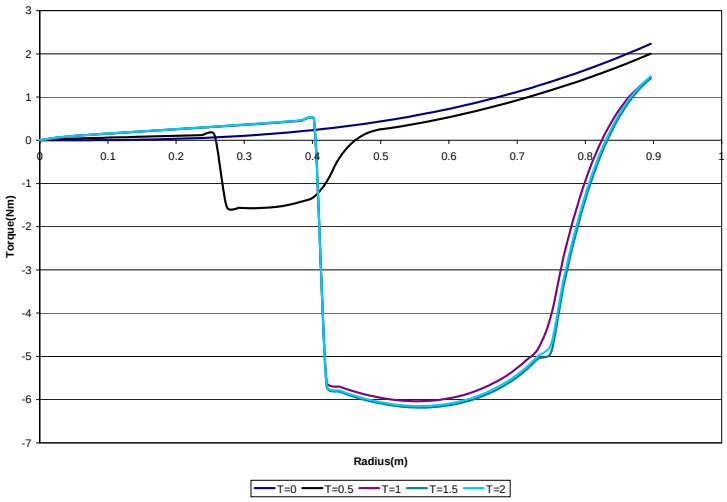

Fig.4 Torque distribution along rotor blade at zero collective pitch.

Torque distribution along the blade span is mainly due to the variation angle of attack. It is defined whether it act as accelerating torque or decelerating torque. Accelerating torque is desired to perform continues main rotor rotation with the help of forward tilt velocity vector. This vector can only be present at high angle of attack that contributed from high descent velocity. Because of that the accelerating torque area or driving region area are getting bigger with time manoeuvre. This situation continues until the total torque from both side are equal in magnitude, means steady rate of descent is achieved.

In order to produce lift the blade must have a positive angle of attack with respect to resultant air flow and so it is common for the blade to have positive pitch in autorotation. Therefore, reducing angle of attack at beginning autorotation will decrease the lift produced by the blade. However relative inflow has an upward component that increases the positive angle of attack by increases in descent velocity. As can been seen in figure 5, the development of the thrust is increased with time. In autorotation manoeuvre, the thrust is started to develop about at the centre of the blade. Conversely, the region near the root experience very high angle of attack that exceed maximum angle stall. Therefore excessive thrust drop is depicted at that figure. In the region near the tip, a small angle of attack is been produced. This is because high induced velocity occurred in this region that make the total upward velocity is small. Consequently, just a small positive angle of attack can be produced to create the thrust.

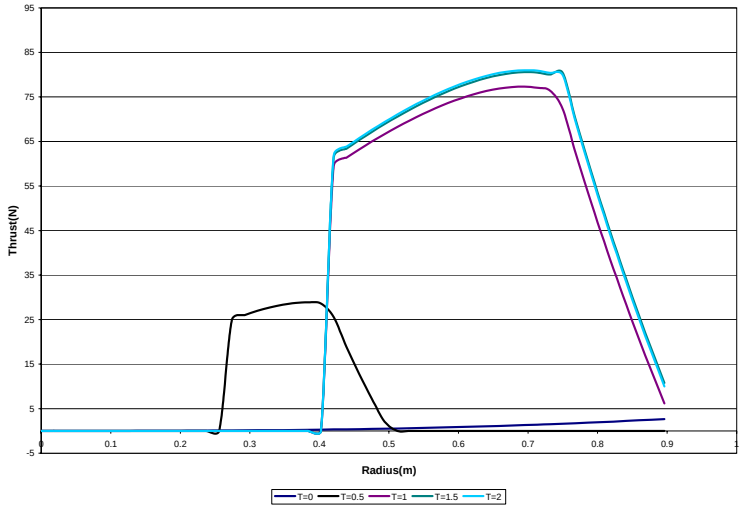

Fig.5 Thrust distribution along rotor blade at zero collective pitch.

Final collective pitch correction play important role in the distribution of torque and thrust. Fixed collective pitch autorotation is possible to keep rotor rotating and to perform safe landing. Figure 6 and 7 show the distribution of torque and thrust at fixed hovering collective pitch. Driving region seems to move away from the blade. At beginning autorotation, driving region developed at 30 percent cord starting to shift to the tip. The same situation is happened in the thrust distribution. This condition continues until no more driving region is developed and helicopter experienced blade stall. At this time safe landing is possible to make because of main rotor had stopped and helicopter descent at free fall velocity.

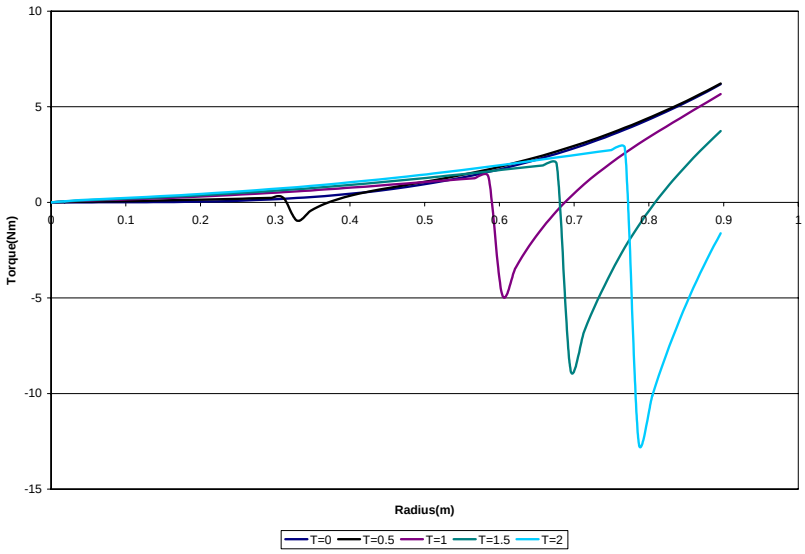

Fig.6 Torque distribution along rotor blade at hovering collective pitch.

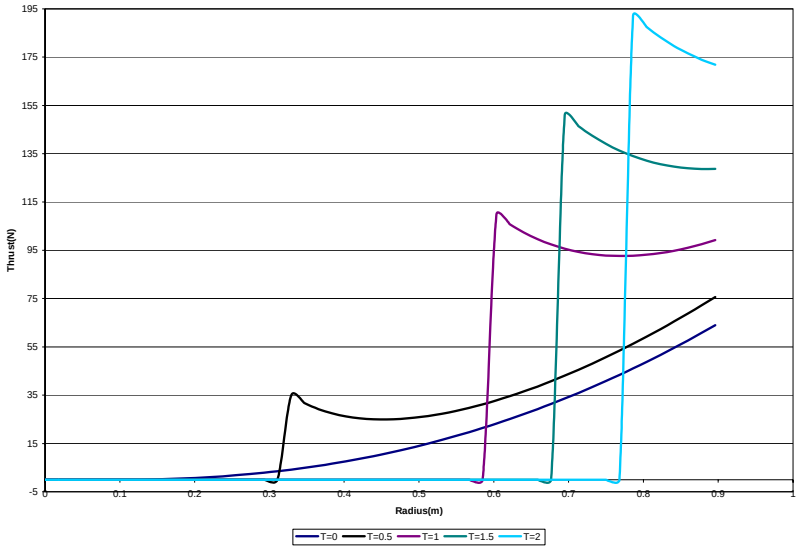

Fig.7 Thrust distribution along rotor blade at hovering collective pitch.

4. Summary

It has been demonstrated that an appropriate BEMT with non uniform circularly symmetrical method may be used to provide characteristics of UAV helicopter autorotation transition performances. This paper shown, that accelerating torque can be defined by the area of driving region on the blade. This driving region is mainly due to inflow angle of attack where is changing in this region will help to keep the main rotor rotating. Hence, autorotation safe landing can be improved by expending this driving region. Therefore, further study on blade modification by expanding chord length at the centre of the blade is seemed possible to increase autorotation characteristics then make a safe landing.

Acknowledgment

This study has been sponsored by *Pembangunan Tabung Perindustrian* (PTP) University of Technology Malaysia.

References

[1] Aponso, B. L., Lee, D., Bachelder, E. N., 2005. Automated Autoratation for Unmanned Rotorcraft Recovery, *AHS International Specialists Meeting on Unmanned Rotorcraft,* Chandler, AZ, January 18-20.
[2] Skews, B. W., 1998. Autorotation of Polygonal Prisms with an Upstream Vane, *Journal of Wind Engineering,* 73: 145-158.
[3] Yeow, A., and Lee, N., 1985. Optimal Landing of a Helicopter in Autorotation. Master Thesis. Stanford University.
[4] Prouty, J., W., 1986. Helicopter Performance, Stability, and Control. Boston, Massachusetts: PWS Publisher.
[5] Shi-cun, W., 1990. Analytical Approach to the Induced Flow of a Helicopter Rotor in vertical Descent, Journal of the American Helicopter Soceity, 1: 92-98
[6] Leishman, J. G., Bhagwat, M. J., and Ananthan, S., 2002. Free-Vortex Wake Predictions of the Vortex Ring State for Single-Rotor and Multi-Rotor Configurations, *Annual Forum and Technology Display of AHS International*, Montreal, Canada, June 11-13.
[7] Leishman, J. G., 2000. Principles of Helicopter Aerodynamics. Cambridege, UK: Cambridge University Press.
[8] Heyson, H. H., 1956. Development of Induced Velocity Fields by superposition, *NASA Technical Note,* NACA TN 3690.
[9] Slaymaker, S. E., Lynn, R. R., and Gray, R. B., 1952. Experimental Investigation of Transition of a Model Helicopter Rotor from Hovering to Vertical Autorotation, *NASA Technical Note,* NACA TN 2648.